Student thesis series INES nr 681

Case study in observing the vegetation-albedo feedback during climate change in the Sahel

Daniel Kirk

2024
Department of
Physical Geography and Ecosystem Science
Lund University
Sölvegatan 12
S-223 62 Lund
Sweden

Daniel Kirk (2024).
Case study in observing the vegetation-albedo feedback during climate change in the Sahel
Bachelor degree thesis, 15 credits in Physical Geography and Ecosystem Analysis
Department of Physical Geography and Ecosystem Science, Lund University

Level: Bachelor of Science (BSc)

Course duration: *January* 2024 until *June* 2024

Disclaimer

Case study in observing the vegetation-albedo feedback during climate change in the Sahel

---

Daniel Kirk

Bachelor thesis, 15 credits, in Physical Geography and Ecosystem Analysis

Supervisor: Vaughan Phillips
Department of Physical Geography and Ecosystem Analysis

Exam committee:
Anna Terskaia, Department of Physical Geography and Ecosystem Analysis
Torbern Tagesson, Department of Physical Geography and Ecosystem Analysis

Acknowledgements

First and foremost, I would like to thank my supervisor Dr. Vaughan Phillips for his support, expertise, and useful advice and guidance. Furthermore, for his assistance with the climate feedback theory lecture notes which provide the basis for the mathematics found in the introduction. NCEP-NCAR Reanalysis 1 data provided by the NOAA PSL, Boulder, Colorado, USA, from their website at https://psl.noaa.gov. MODIS Albedo and NDVI data provided by NASA through the AppEEARS application https://appeears.earthdatacloud.nasa.gov.

Abstract

Due to drying trends in the tropical and subtropical areas there is a potential for significant vegetation loss. As this occurs previous literature has predicted significant increases in desert area, further exacerbated by vegetation-albedo feedback with radiation in climate change. This study analyses this phenomenon at a smaller local scale over an area of 100 x 100 km in the middle of Chad. The aim is to provide a method for examining climate feedbacks at these small spatial scales. Using NDVI and albedo data in addition to climate variables, an overall decrease in fractional vegetation area is observed within the study area from 0.083 to 0.068 over 20 years from 2001 to 2023. This implies a relatively strong local vegetation-albedo radiation feedback of $Y = 1.24 \pm 0.25\, W/m^2/K$, representing a negative feedback loop in the climate system.

Table of Contents

Contents

1 Introduction

1.1 Overview of vegetation-albedo feedback during global warming

As argued by Held and Soden (2006) there has been and will continue to be a worsening of extremes in the climate during global warming. Specifically, that dry areas get drier and wet areas get wetter. This is due to the exponentially increasing amount of water vapour stored in the lower troposphere, which the atmospheric circulation is unable to keep up with as its subsidence is limited by radiative cooling aloft. It results in a slowing of mass circulation in the atmosphere (Held, Soden, 2006). This means that in many of the areas which experience heavy lifting or subsidence those processes will be slowed. The result of which is heavier precipitation in areas which already had high precipitation and less precipitation in areas with low precipitation (Held, Soden, 2006).

The climate system is driven by the net radiation entering the top of the atmosphere. When the net radiation deviates from zero, there will be a global warming or cooling that then re-arranges processes that somehow depend on temperature. As the climate responds to this perturbation of the net radiation, these "feedback processes" may then alter the net radiation and global mean temperature to reach a new equilibrium. Such feedback processes include clouds, ice, and the water vapour feedback. (Cess, et al., 1990)

The drying during global warming in dry regions noted above also contributes to feedback loops. As described by Zeng and Yoon (2009) a possible interaction exists between the albedo of vegetation and the climate in desert areas. The feedback proposed by that paper is as follows. Due to the overall drying in the subtropics there will be a decrease in vegetation caused by the decrease in soil moisture and high heat stress. This results in a higher albedo, which decreases precipitation, further decreasing the extent of vegetation. This decrease in precipitation could also be mechanistically similar to an inverse of the precipitation recycling in tropical rainforests (Langenbrunner, et al., 2019) (Zeng, Neelin, 1999). Where due to less radiation being absorbed at the surface there is less local lifting and evapotranspiration. Zeng and Yoon also predict a large increase in hot desert areas due to the inclusion of this feedback mechanism, at a total of 34 percent as opposed to the 10 percent expansion proposed by the IPCC models of the time.

A study by Bony and DuFresne from 2006 also looks into feedbacks of a different nature. Investigating the effects of variance in cloud feedbacks by calculating the effects of different cloud types on cloud radiative forcing in ocean environments to determine the sensitivity of the cloud radiative feedback to different cloud types. Similarly, this study will examine the effects of the vegetation albedo feedback locally rather than globally.

1.2 Aim and research questions

The aim of this study is to examine the effects of the vegetation albedo feedback at a local scale within the Sahel, and to test the method proposed herein as a viable option for investigating different feedback loops.

- Is the vegetation-albedo feedback positive or negative in the study area?
- How strong is the vegetation-albedo feedback in the study area?

2 Background

2.1 Concepts of climate feedbacks and net radiation

It is of relevance to quantify what exactly a feedback in the climate system entails. Fundamentally a radiative feedback is the balance between surface air temperature and top of atmosphere (TOA) net radiation mediated by a specific process (Cess, et al., 1990). Feedbacks are investigated as a separated link via one process and do not represent a simulation of the entire climate system (Gregory, Andrews, 2016). There are fundamentally two different forms of climate feedback, a positive feedback which results in the change to a system being reinforced, and a negative feedback which results in the change to a system being opposed. One useful example of a positive feedback is the ice melt albedo feedback. In which, due to a reduction in ice coverage, the planet's albedo decreases resulting in more radiation being absorbed by the surface, further contributing to warming trends (Budyko, 1969).

The following mathematical framework is supported by Gregory and Andrews (2016), Cess, et al. (1990), and Cess (1976).

To understand these feedbacks, it is important to consider the earth as a system, as they are globally applied processes. At the top of the atmosphere the net radiation balance between all long and shortwave fluxes across the globe must be zero when that system is in equilibrium. The TOA net radiation (Q) can then be defined globally as:

$$Q = Incoming\ Shortwave\ radiation - Outgoing\ Shortwave\ radiation - Emitted\ Longwave\ radiation$$

This net radiation is the strongest driver of climate change, in a stable state however it is always very near to zero. An extremely simple climate model would then be that the change in surface air temperature with respect to time (dT_s/dt) is proportional to the net radiation (Q) globally, or:

$$\frac{dT_s}{dt} \propto Q \quad (1)$$

One can then say that when a forcing (or instantaneous external modification) is made to the system, such as a volcanic eruption, the initial value of Q is the value contributed by the forcing Q_0. From this there will be a response via various climate feedback processes to work to balance out the change in net radiation, which can be represented as:

$$Q = Q_0 - Y\Delta T_s \quad (2)$$

Where Y is the climate feedback parameter, representing a sum of all climate feedback processes, and ΔTs is the change in global mean surface air temperature. Negative feedbacks are defined by a positive Y value as they oppose the change to the net radiation, and positive feedbacks are defined by a negative Y value. Therefore, globally, the total value of Y has to be positive because there must be a net negative feedback across the entire climate system (the energy in the system can obviously not increase infinitely with no input).

Initially we can then say that ΔT_s and Q are equal to zero, and that for any change made as time goes to infinity the net radiation will return to zero at a new temperature. With these two assumptions we can also say that in that new equilibrium:

$$\Delta T_s = \frac{Q_0}{Y} \quad (3)$$

So, for example, if the forcing by an instantaneous doubling of CO_2 is $Q_0 = 4$ W/m^2, and the total Y value is 0.9 to 2.4 W/m^2/K we would get a change of temperature in the new equilibrium ranging approximately from $\Delta T_s = 2$ to 4 K.

Y is then defined as:

$$Y = -\frac{dQ}{dT_s} \quad (4)$$

The negative sign is applied to remain consistent with the definition of negative and positive feedbacks. This can then be separated out to investigate individual feedbacks within the climate system by analysing different variables. Since $Q = Q(T_S, X_1, X_2, \dots)$, then by the chain rule we get:

$$Y = \sum_{i=1} Y_i = -\sum_{i=1} \frac{\partial Q}{\partial X_i} * \frac{dX_i}{dT_s} + \frac{\partial Q}{\partial T_s} \quad (5)$$

Where X_i is a specific variable characterizing a feedback process, and the second term is a term representing black-body feedback. Black-body feedback being a process in which by absorbing radiation the earth's surface acts as a black body emitter in accordance with Stefan-Boltzmann law (negative feedback) (Cronin, Dutta, 2023). Some examples of feedbacks are the ice-melt albedo feedback, water vapour feedback (in which water vapour acts as a greenhouse gas, positive) (Hall, Manabe, 1999), blackbody feedback, and many others. If one wishes to investigate an individual non-cloud related feedback they must avoid the presence of clouds as much as possible due to the fact that clouds and their feedback processes are the strongest local climate modifier (Ceppi, et al., 2017).

It is important to investigate the effects of these individual feedbacks as even small contributions to the climate system can add up to large effects. This will be done here by examining the feedback at a local scale as opposed to attempting to evaluate the feedback for the entire globe.

Finally, it is of relevance to define the average global solar insolation as $S = S_0/4$. Where S_0 is the flux in space normal to the solar beam and 4 is derived from the ratio of a spherical surface to the surface area of a circle of the same size.

3 Data

Table 1: Details for the datasets used in the analysis and calculation of the climate feedback parameter.

Dataset	Air Temperature (deg C)	Downward Solar Radiation (W/m^2)	Albedo (Unitless)	NDVI (Unitless)
Source	NCEP-NCAR reanalysis 1 (Kalnay, et al., 1996)	NCEP-NCAR reanalysis 1 (Kalnay, et al., 1996)	MODIS MCD43A3.061 (Schaaf, Wang, 2021)	MODIS MOD13A1.061 (Didan, 2021)
Projection System	WGS84	WGS84	Sinusoidal	Sinusoidal
Scale Factor	N/A	N/A	0.001	0.0001
Time Span	29/12-04/01 and 07/06-13/06 for years 2001, 2010, and 2023 (note: January week starts in December of the previous year)	29/12-04/01 and 07/06-13/06 for years 2001, 2010, and 2023 (note: January week starts in December of the previous year)	29/12-04/01 and 07/06-13/06 for years 2001, 2010, and 2023 (note: January week starts in December of the previous year)	Sixteen-day average represented on the 9th day of the 16 day period, those dates being January 1st and June 10th of 2001, 2010, and 2023
Spatial Resolution	2.5 x 2.5 degrees	2.5 x 2.5 degrees	500 x 500 meters	500 x 500 meters
Data Format	NetCDF	NetCDF	GeoTIFF	GeoTIFF
Additional Notes	Daily values for 1000 mbar pressure level	Daily values for "Nominal Top of Atmosphere"	Daily values, Black Sky Albedo	Sixteen-day average
Retrieved from	NOAA PSL	NOAA PSL	NASA AppEEARS web tool (AppEEARS team, 2024)	NASA AppEEARS web tool (AppEEARS team, 2024)

Acronyms:

NDVI – Normalized Difference Vegetation Index

NCEP-NCAR – National Centers for Environmental Prediction and National Center for Atmospheric Research

MODIS – Moderate Resolution Imaging Spectroradiometer

NetCDF – Network Common Data Form

GeoTIFF – Georeferenced Tagged Image File Format

NOAA PSL – National Oceanic and Atmospheric Administration Physical Sciences Laboratory

NASA AppEEARS – National Aeronautics and Space Administration Application for Extracting and Exploring Analysis Ready Samples

4 Method

4.1 Study area

The study area selected is in the middle of Chad in the Sahel. It covers an area of roughly 100 x 100 km and has few notable features aside from the town of Ati which is the largest human settlement within the study area. The climate in Chad is hot and semi-arid with temperatures ranging from 20-35 degrees Celsius and annual rainfall up to 500mm varying across the country (Sarr, et al., 2015).

4.2 Model of vegetation interaction with shortwave radiation

Due to the nature of albedo as a reflectance of shortwave radiation, and the time constraints of this project, it was decided to focus only on the net shortwave radiation. The climate feedback parameter was calculated by applying the global model discussed in the background section (eq. 1-5) in a simplified capacity using variables for the study area. Those variables being TOA downward solar radiation, albedo, surface air temperature, and NDVI derived fractional vegetation area.

To do this we begin with:

$$Q_{SW} = S(1 - \alpha - \alpha_{atm}) \quad (6)$$

Where Q_{sw} is the TOA net shortwave radiation, simplified as a balance between the incoming solar radiation (S), ground albedo (α), and atmospheric albedo (α_{atm}), as the long wave radiation is not being accounted for. The atmospheric albedo will be addressed in the discussion, and the ground albedo is then calculated by using:

$$\begin{aligned} \alpha &= A_V\alpha_V + (1 - A_V)\alpha_d \\ &= A_V(\alpha_V - \alpha_d) + \alpha_d \end{aligned} \quad (7)$$

Where α is the ground albedo, which has been separated out into vegetative albedo (α_v) and barren or "desert" albedo (α_d) using the fractional vegetation area (A_v). Inserting equation 7 into equation 6 and taking the partial derivative (defined by all other feedback processes being held constant) with respect to fractional vegetation area results in the first term of Y:

$$\frac{\partial Q_{SW}}{\partial A_V} = -S(\alpha_V - \alpha_d) \quad (8)$$

The second term of the climate feedback parameter can then be calculated much more simply, by creating a scatterplot of the fractional vegetation area with respect to the surface air temperature, creating a linear line of best fit, and taking its slope as dA_v/dT_s.

To find the fractional vegetation area, one then needs a measure of vegetation and its extent in the study area. One potential measurement of this is NDVI, which is a ratio between the reflected near infrared (NIR) radiation, and radiation reflected in the red-light band, as can be seen in equation 9. This is because vegetation reflects light very heavily in the NIR band and absorbs light heavily in the red band (Knipling, 1970). For this any reading below 0.2 is often considered to be barren. (El-Gammal, et al., 2014) (Huang, et al., 2021)

$$NDVI = (NIR - Red)/(NIR + Red) \quad (9)$$

4.3 Calculation of fractional vegetation area from NDVI

Finally, the method for calculating fractional vegetation area from NDVI is as follows. A paper from Carlson and Ripley (1997) states that the fractional vegetation area is approximately equal to the square of the scaled NDVI, or:

$$A_v \approx N°^2 \quad (10)$$

Where A_v is the fractional vegetation area and N°, the scaled NDVI, can be expressed as:

$$N° = \frac{NDVI - NDVI_0}{NDVI_S - NDVI_0} \quad (11)$$

Where NDVI is the NDVI reading for a cell within the study area, $NDVI_S$ is the NDVI value for $A_v = 1.0$ (in this case assumed to be the cell with the highest NDVI), and $NDVI_0$ is the NDVI value for the lowest bare soil reading (assumed to be the cell with the lowest NDVI).

4.4 Data Analysis

Using ArcGIS Pro 2.7 (ESRI, 2020) the rasters were projected from their original coordinate systems into WGS1984 Web Mercator (Auxiliary sphere) using the project raster tool.

Because the data for air temperature and downward solar radiation had much coarser spatial resolution than the study area's extent, the values for these variables were taken directly by sampling the cells in which the study area resided.

For each season, the NDVI mappings had to be corrected with their associated scale factor using the raster calculator tool. Following this the fractional vegetation area was calculated directly from NDVI according to equations 11 and 12 using the raster calculator. As this mapping showed the fractional vegetation area on a per cell basis the mean of all cells within the study area was taken as the fractional vegetation area for the whole study area. The fractional vegetation area mappings were then reclassified to create a layer containing only the cells with a fractional vegetation area of 0.05 or lower and assign them a value of 1. All other cells were assigned a value of NODATA. This was done to create a layer that could be used to separate out the cells with predominantly little or no vegetation.

Similarly, for each season, the albedo mappings were corrected with their associated scale factor using the raster calculator. As they were daily values, they were first averaged on a per cell basis for the seven-day period they fell into. This created another albedo mapping which was the average of all seven days. The mean value of albedo within all the cells in the study area was then taken as the albedo for the whole study area. The new albedo mapping was then multiplied with the separation layer created from the fractional vegetation data to get a value for the "desert" albedo within the study area (again, a mean). This was possible as both the NDVI and albedo data shared exactly a cell size, cell location, and spatial extent.

The data was then processed in Excel (Microsoft Corporation, 2018) as follows. From the study area albedo, the "desert" albedo, and the fractional vegetation area the vegetative albedo value (α_v) was calculated according to the following equation.

$$\alpha_V = \frac{\alpha_{study\ area} - (1 - A_V)\alpha_d}{A_V} \quad (12)$$

This equation was derived from the fact that both any cell within the study area and the entire study area itself follow the relationship outlined in equation 7.

Following this all values were then averaged to the yearly values seen in tables 2, 3, and 4. Using these values and equations 5 and 8 the feedback parameter for the vegetation-albedo interaction was calculated. The values for fractional vegetation area were plotted against the surface temperature in a scatterplot and a line of best fit was taken, the slope of which fulfilled the second half of equation 5.

5 Results

Table 2: Climate values obtained from NCEP-NCAR Reanalysis 1 for calculating the climate feedback parameter for each of the three sampled years within the study area.

	2001	2010	2023
Air temperature (deg C)	28.0	29.9	28.8
Downward solar radiation (W/m^2)	389	389	389

Table 3: Fractional vegetation areas calculated from NDVI for the study area in all three of the sampled years.

	2001	2010	2023
Fractional vegetation area (Unitless)	0.083	0.058	0.068

Table 4: Average albedo values for the study area, and the vegetated and barren areas in the study area. The albedo values for barren areas are averaged over a large number of cells, and the albedo values for vegetated areas are calculated back from that number and the mean albedo of the study area.

	2001	2010	2023
Vegetation (Unitless)	0.165	0.126	0.154
Non-vegetation (Unitless	0.389	0.413	0.387
Study area albedo	0.370	0.396	0.371

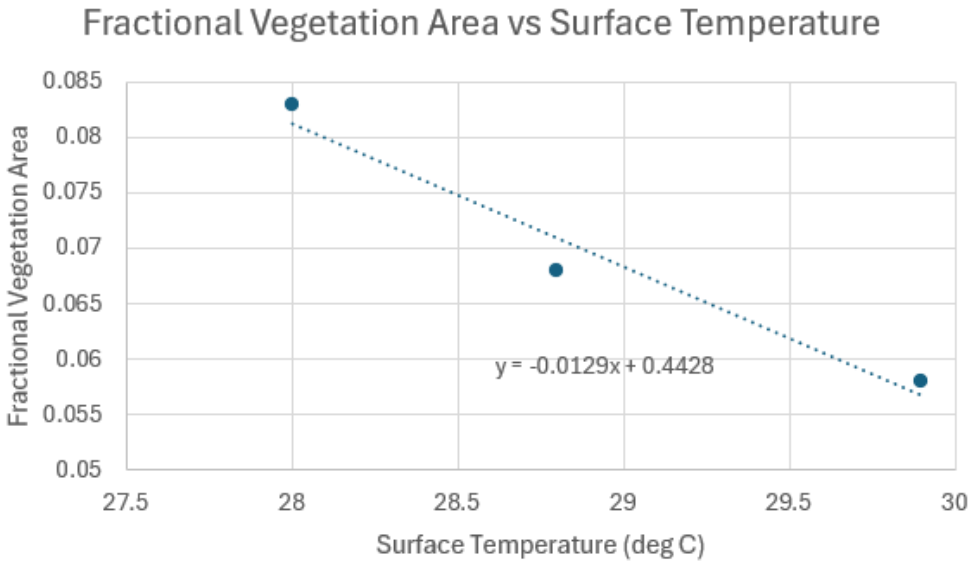

Fig. 1 Graph of fractional vegetation area plotted against surface air temperature (deg C) for each of the sampled years within the study area, trendline and equation for trendline are included as they are necessary for the climate feedback parameter calculation.

The climate feedback parameter calculated below indicates that for the study area the feedback is negative.

Calculation for Y using averaged values over all three of the sampled years:

$$\frac{\partial Q_{SW}}{\partial A_V} = -S(\alpha_V - \alpha_d)$$
$$= -389(0.148 - 0.396)$$
$$= 96.471$$
$$Y = -\frac{\partial Q}{\partial A_V} * \frac{dA_V}{dT_s}$$
$$Y_{veg-albedo} = -96.471 * -0.0129$$
$$Y_{veg-albedo} = 1.24\ W/m^2/K$$

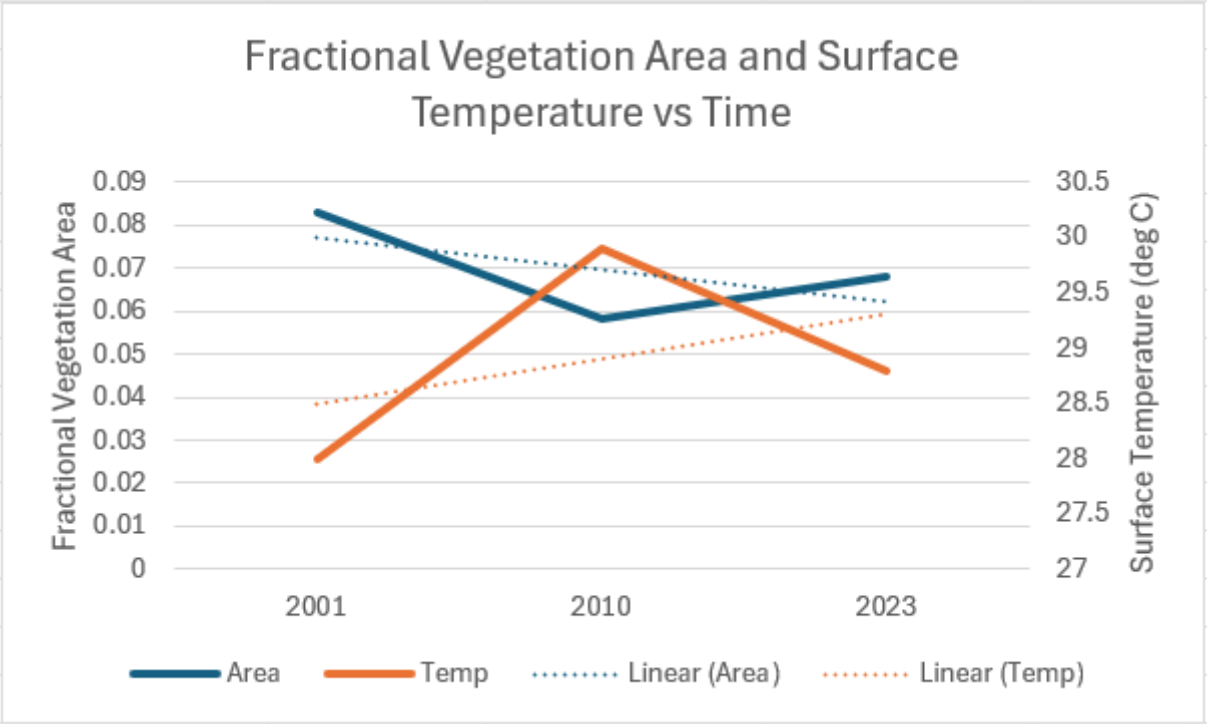

Fig 2. Graph of fractional vegetation area (unitless) and surface air temperature (deg C) as a function of time within the study area, trendlines included to show slight overall warming and vegetation loss trends.

6 Discussion

6.1 Interpretation of results and uncertainties

It is clear from the calculated feedback parameter that the vegetation albedo feedback within the study area is a negative feedback. This means that as the vegetation area is decreasing the albedo of the study area somewhat increases resulting in more radiation being reflected out of the system and a slowing of vegetation loss. Although, this is only a relatively small increase in albedo from 0.370 to 0.371. In any case, it is possible that the decrease in vegetation also results in less evapotranspiration occurring in the area as there is less vegetation present (Pereira, et al., 1999). This is relevant as it could also affect the water vapour feedback (Hall, Manabe, 1999) which is a positive feedback. In simple terms we can say that as vegetation is lost the study area becomes less effective at trapping radiation and *potentially* less effective at contributing to other warming effects. Instead, it becomes a slightly more efficient reflector of radiation.

It is worth noting that for the study area the calculated feedback parameter also appears to be a relatively strong feedback. In comparison with the feedback values found in table 10 and 11 in Cess, et al. (1990), which range from feedback parameters of absolute value 0.05 up to 3, a feedback parameter of 1.24 $W/m^2/K$ is substantial. Of large importance is that this value only corresponds to the vegetation albedo feedback within the study area and Sahel and not necessarily the vegetation albedo feedback globally.

Regarding whether the study area is representative of the Sahel is potentially contentious. One could say that a 100 by 100-kilometer area is not very large in comparison to the rest of the Sahel, which spans across the width of Africa and extends from the southern edge of the Sahara to many hundreds of kilometers south (Mirzabaev, et al., 2021). This, however, is of less concern due to the relatively central location of the study area in the continent and the general homogeneity of temperature and climate gradients in the tropics (Sobel, et al., 2001).

Given that vegetation extent is likely precipitation limited in the area it would be necessary to examine these results alongside precipitation. However, there is a lack of both direct monitoring in the region and relevant global precipitation data that covers the time span and location. It is therefore sufficient to say that the study could be improved upon by finding precipitation data that functions for the area.

One possible source of uncertainty is the choice of datasets used, specifically for the NDVI and albedo. The albedo values came from the MCD43A3.061 albedo product (Schaaf, Wang, 2021) using the black sky albedo values calculated for the NIR radiation band. This was chosen because the black sky albedo product should be closer to clear sky conditions than the white sky albedo product. The NIR band was chosen as this should be the band in which vegetation reflects the most radiation, likely making it more representative of the vegetation cover in the area (Knipling, 1970).

There are however, some notable issues. The first of which is that the black sky albedo (directional hemispherical reflectance) is not a direct clear sky albedo. Instead, it is an albedo calculated for a situation in which there is no diffuse component and therefore could only be used as a proxy for clear sky. Whereas white sky albedo (bihemispherical reflectance) is a

situation in which the maximum amount of diffusion is present. (Kimes, Sellers, 1985) (Lewis, Barnsley, 1994)

Meaning that while choosing black sky should result in a more direct reading of the albedo, it does not necessarily guarantee the exclusion of clouds. Which is important as clouds are a very strong climate modifier and their inclusion in the data could mischaracterize results (Ceppi, et al., 2017).

It is also worth noting that choosing to use the NIR band for albedo comes with downsides. Importantly this band of the satellite sensor cuts out visible light and only covers a band width from 0.7-5.0 μm out of the total 0.3-5.0 μm available in the MODIS data (Schaaf, Wang, 2021). This should, as mentioned, be more representative of vegetation as it focuses more on the NIR reflectance but that comes with the downside of potentially misrepresenting other surfaces. Which means that, for example, sand could be reflecting more radiation than it appears to be in the albedo mappings. This is a weakness as it has a direct impact on the reliability of the calculated climate feedback parameter. Many of these issues should, however, be lessened by averaging the albedo readings over a longer period.

Another possible point of contention with the albedo data is the calculation of the "desert" albedo and vegetative albedo. Given that the "desert" albedo is calculated from a reclassification very near to the overall mean fractional vegetation area one could argue that this makes it less representative of bare soil. This, however, is less of an issue as the study area is for the most part dominated by bare soil. By necessity this study's method relies on this splitting of the study area into a vegetated area and a non-vegetated area. This is, however, not necessarily the ground truth. There are certainly human settlements in the area which means that other materials beyond vegetation and bare soil are present, even if in lower quantities than either.

Finally, as featured in eq 6, the last potential source of error in the ground albedo itself is the contribution of in atmosphere aerosols and clouds to the albedo reading (Bauer, Menon, 2012). As mentioned previously, this should be at least mitigated by the choice to use black sky albedo over white sky albedo. It is, however, possible that there is still contribution from these effects in the albedo values as calculated.

It is also worth investigating the applicability of the NDVI data used. While NDVI is useful as a proxy for vegetation it is not a direct measurement of vegetation cover (Huang, et al, 2021). Converting between NDVI and fractional vegetation area should account for this issue to some extent. However, comparison against other vegetation indices, such as Fraction of Absorbed Photosynthetically Active Radiation (FAPAR), could still yield useful insights into the vegetation cover. In either case if this study is to be replicated it is very worth looking into alternative vegetation indices as they would be useful points of comparison.

Another issue is the time span during which the climate variables were taken. While solar radiation varies very little on a weekly basis, temperature can absolutely vary week to week. This is somewhat accounted for by testing for two different weeks per year, but it would likely be an improvement to take entire months instead as the temperature variation would be lessened.

6.2 Error analysis

The relative error of each of the terms in Y was calculated to be $\frac{\partial Q}{\partial A_V}_{relerror} = 0.114$ and $\frac{dA_V}{dT_S}_{relerror} = 0.086$. For the dA_V/dT_S term this was done using the standard deviation of the differences between the actual values and the line of best fit in fig.1. Whereas for the $\partial Q/\partial A_V$ term the relative error was calculated using the standard deviation of the yearly albedo values. Using these values, we get that the relative error of the Y term is $Y_{relerror} = 0.200$ or 20 percent relative error. We then get that the overall error of Y is $Y_{error} = \pm 0.25\ W/m^2/K$.

One slight issue with this error value is that it was calculated for a small set of data points, meaning that calculating Y over a larger number of data points would likely decrease the error. However, the error is likely more representative then as the method used for calculating the error accounts for variation within the results and not the variation in the datasets. Meaning that having a larger error likely indirectly acts to account to some extent for whatever uncertainties are present in the datasets.

6.3 Possible improvements/future research

One way in which the study could be improved, apart from what has already been mentioned above, is to attempt this method for a larger area. Which would inherently make the results more applicable to the Sahel as a whole. Similarly having a much finer spatial resolution for the datasets would result in more relevant results being generated. However, improving the spatial resolution of the MODIS data would improve the accuracy to a lesser extent as it already has a much finer spatial resolution than the reanalysis data. In addition, using a more detailed time series would also increase the relevancy of the results as they currently only really include six data points and all of these data sets represent continuous data. There also is not any data from any other part of the year than January or June included which means that the applicability of the data to other times of year can't be guaranteed.

This method could be applied in the future to a variety of different feedbacks to investigate how they interact on a smaller scale. It could also be used to continue furthering the understanding of how the vegetation-albedo feedback functions.

7 Conclusions

By using climate variables obtained from reanalysis, albedo and NDVI data from the MODIS satellite, and the proposed model, the feedback between vegetation and albedo in the Sahel can be analysed. This feedback appears to be a negative feedback of relatively high strength which potentially very slightly slows the loss of vegetation in the study area. This comes with a wide variety of uncertainties and further study is needed to elaborate upon the viability of this method for investigating climate feedbacks.

Findings:

- Localised feedback interaction specific Y value of $1.24 \pm 0.25\ W/m^2/K$
- Fractional vegetation area decreases from 0.083 to 0.068 over 20 years from 2001 to 2023

8 References

AppEEARS Team. (2024). Application for Extracting and Exploring Analysis Ready Samples (AppEEARS). Ver. 3.53. NASA EOSDIS Land Processes Distributed Active Archive Center (LP DAAC), USGS/Earth Resources Observation and Science (EROS) Center, Sioux Falls, South Dakota, USA. Accessed May 7, 2024. https://appeears.earthdatacloud.nasa.gov

Bauer, S. E., & Menon, S. (2012), Aerosol direct, indirect, semidirect, and surface albedo effects from sector contributions based on the IPCC AR5 emissions for preindustrial and present-day conditions, *Journal of Geophysical Research: Atmospheres*, 117(D1), D01206, doi:10.1029/2011JD016816

Bony, S., & J.L. Dufresne (2005), Marine boundary layer clouds at the heart of tropical cloud feedback uncertainties in climate models, *Geophysical Research Letters*, 32, L20806, doi:10.1029/2005GL023851

Budyko, M. I. (1969). The effect of solar radiation variations on the climate of the Earth. Tellus A: *Dynamic Meteorology and Oceanography*, 21(5), p.611-619, https://doi.org/10.3402/tellusa.v21i5.10109

Carlson, T., & Ripley, D. (1997) On the relation between NDVI, fractional vegetation cover, and leaf area index, *Remote Sensing of Environment*, 62(3), p.241-252, ISSN 0034-4257, https://doi.org/10.1016/S0034-4257(97)00104-1.

Ceppi, P., Brient, F., Zelinka, M.D. & Hartmann, D.L. (2017), Cloud feedback mechanisms and their representation in global climate models. *WIREs Climate Change*, 8(4), https://doi.org/10.1002/wcc.465

Cess, R. D. (1976). Climate Change: An Appraisal of Atmospheric Feedback Mechanisms Employing Zonal Climatology. *Journal of Atmospheric Sciences*, 33(10), p.1831-1843. https://doi.org/10.1175/1520-0469(1976)033<1831:CCAAOA>2.0.CO;2

Cess, R.D., Potter, G.L., Blanchet, J.P., Boer, G.J., Del Genio, A.D., Deque, M., Dymnikov, V., Galin, V., Gates, W.L., Ghan, S.J., Kiehl, J.T., Lacis, A.A., Le Treut, H., Li, Z.X., Liang, X.Z., McAvaney, B.J., Meleshko, V.P., Mitchell, J.F.B., Morcrette, J.J., Randall, D.A., Rikus, L., Roeckner, E., Royer, J.F., Schlese, U., Sheinin, D.A., Slingo, A., Sokolov, A.P., Taylor, K.E., Washington, W.M., Wetherald, R.T., Yagai, I., & Zhang, M.H. (1990). Intercomparison and interpretation of climate feedback processes in 19 atmospheric general circulation models. *Journal of Geophysical Research*, 95, p.16601-16615, doi:10.1029/JD095iD10p16601

Cronin, T. W., & Dutta, I. (2023). How well do we understand the Planck feedback? *Journal of Advances in Modeling Earth Systems*, 15(7), e2023MS003729. https://doi.org/10.1029/2023MS003729

Didan, K. (2021). MODIS/Terra Vegetation Indices 16-Day L3 Global 500m SIN Grid V061. NASA EOSDIS Land Processes Distributed Active Archive Center. Accessed 2024-04-18 from https://doi.org/10.5067/MODIS/MOD13A1.061. Accessed April 18, 2024.

El-Gammal, M.I., Ali, R.R., & Abou Samra, R.M. (2014). NDVI Threshold Classification for Detecting Vegetation Cover in Damietta Governorate, Egypt. *Journal of American Science*, 10(8), p.108-113.

Esri. (2020). ArcGIS Pro 2.7. Redlands, CA: Environmental Systems Research Institute.

Gregory, J. M., & Andrews, T. (2016), Variation in climate sensitivity and feedback parameters during the historical period, *Geophysical Research Letters*, 43(8), p.3911–3920, doi:10.1002/2016GL068406.

Hall, A., & Manabe, S. (1999). The Role of Water Vapor Feedback in Unperturbed Climate Variability and Global Warming. *Journal of Climate*, 12(8), p.2327-2346. https://doi.org/10.1175/1520-0442(1999)012<2327:TROWVF>2.0.CO;2

Held, I, & Soden, B. (2006). Robust responses of the hydrological cycle to global warming. *Journal of Climate*, 19, p.5686-5699. https://www.gfdl.noaa.gov/bibliography/related_files/ih0601.pdf

Huang, S., Tang, L., Hupy, J.P., Wang, Y., & Shao, G. (2021). A commentary review on the use of normalized difference vegetation index (NDVI) in the era of popular remote sensing. *Journal of Forestry Research*, 32, p.1–6, https://doi.org/10.1007/s11676-020-01155-1

Kalnay, E., Kanamitsu, M., Kistler, R., Collins, W., Deaven, D., LS, Gandin, Iredell, M., Saha, S., White, G., Woollen, J., Zhu, Y., Chelliah, M., Ebisuzaki, W., Higgins, W., Janowiak, J., C, K., Ropelewski, C., Wang, J., & Leetmaa, A. (1996) The NCEP/NCAR 40-year reanalysis project, *Bullet of the American Meteorological Society*, 77, p.437-470

Kimes, D.S., & Sellers, P.J. (1985). Inferring hemispherical reflectance of the earth's surface for global energy budgets from remotely sensed nadir or directional radiance values, *Remote Sensing of Environment*, 18(3), p.205-223, ISSN 0034-4257, https://doi.org/10.1016/0034-4257(85)90058-6.

Knipling, E.B. (1970) Physical and physiological basis for the reflectance of visible and near-infrared radiation from vegetation, *Remote Sensing of Environment*, 1(3), p.155-159, ISSN 0034-4257, https://doi.org/10.1016/S0034-4257(70)80021-9

Langenbrunner, B., Pritchard, M. S., Kooperman, G. J., & Randerson, J. T. (2019). Why does Amazon precipitation decrease when tropical forests respond to increasing CO2?, *Earth's Future*, 7(4), p.450–468. https://doi.org/10.1029/2018EF001026

Lewis, P., & Barnsley, M. J. (1994). Influence of the sky radiance distribution on various formulations of the earth surface albedo, in *Proc. Conf. Phys. Meas. Sign. Remote Sens.*, Val d'Isere, France, pp. 707-715.

Microsoft Corporation. (2018). Microsoft Excel. Retrieved from https://office.microsoft.com/excel

Mirzabaev, A., Sakketa, T. G., Sylla, M., Dimobe, K., Sanfo, S., Admassie, A., Abebaw, D., Coulibaly, O., Adamou, R., Ibrahim, B., Bonkaney, A. L., Seyni, A., Idrissa, M., Olayide, O., Faye, A., Dieye, M., Diakhaté, P., Beye, A., Sall, M., & von Braun, J. (2021). Land, Climate, Energy, Agriculture and Development in the Sahel: Synthesis Paper of Case Studies Under the Sudano-Sahelian Initiative for Regional Development, Jobs, and Food Security. *SSRN Electronic Journal*. 10.2139/ssrn.3769155.

Pereira, L.S., Perrier, A., Allen, R.G, & Alves, I. (1999) Evapotranspiration: Concepts and Future Trends. *Journal of Irrigation and Drainage Engineering.* 125(2), p.45-51. doi:10.1061/(ASCE)0733-9437(1999)125:2(45)

Sarr, B., Atta, S., Ly, M., Salack, S., Ourback, T., Subsol, S., & George, D. A. (2015). Adapting to climate variability and change in smallholder farming communities: A case study from Burkina Faso, Chad and Niger. *Journal of Agricultural Extension and Rural Development*, 7(1), p.16-27.

Schaaf, C., & Wang, Z. (2021). MODIS/Terra+Aqua BRDF/Albedo Daily L3 Global - 500m V061. NASA EOSDIS Land Processes Distributed Active Archive Center. Accessed 2024-05-07 from https://doi.org/10.5067/MODIS/MCD43A3.061. Accessed May 7, 2024.

Sobel, A. H., Nilsson, J., & Polvani, L. M. (2001). The Weak Temperature Gradient Approximation and Balanced Tropical Moisture Waves. *Journal of the Atmospheric Sciences*, 58(23), p.3650-3665. https://doi.org/10.1175/1520-0469(2001)058<3650:TWTGAA>2.0.CO;2

Zeng, N., & Neelin, J. D. (1999). A Land–Atmosphere Interaction Theory for the Tropical Deforestation Problem. *Journal of Climate*, 12(3), p.857-872. https://doi.org/10.1175/1520-0442(1999)012<0857:ALAITF>2.0.CO;2

Zeng, N, & Yoon, J. (2009). Expansion of the world's deserts due to vegetation-albedo feedback under global warming. *Geophysical research letters*, 36(17). doi:10.1029/2009GL039699

9 Appendix

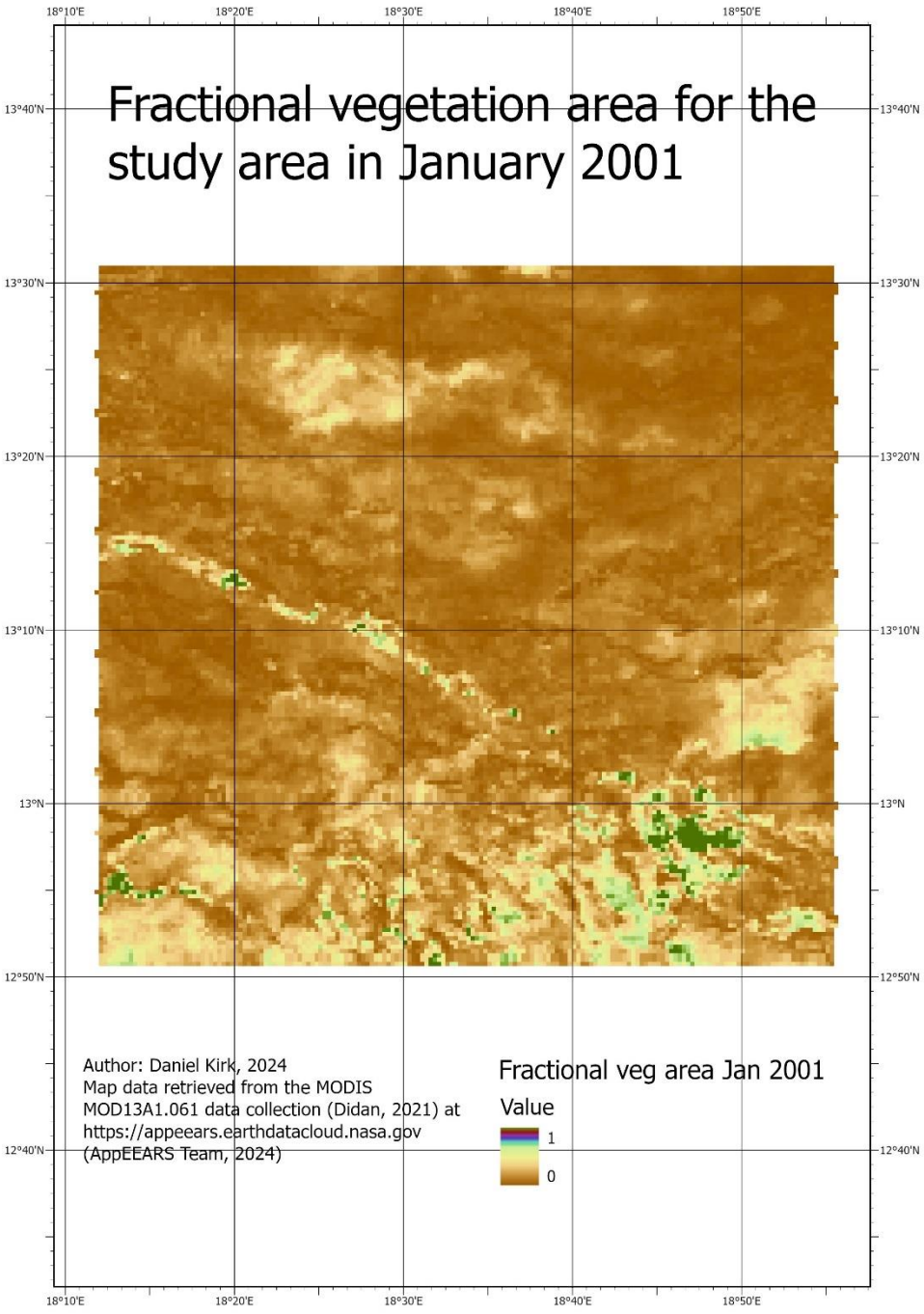

Map 1. Map showing the fractional vegetation area for each 500x500m cell in the study area for January 2001. The map shows the general extent and location of vegetation cover in the study area at the time it was sampled.

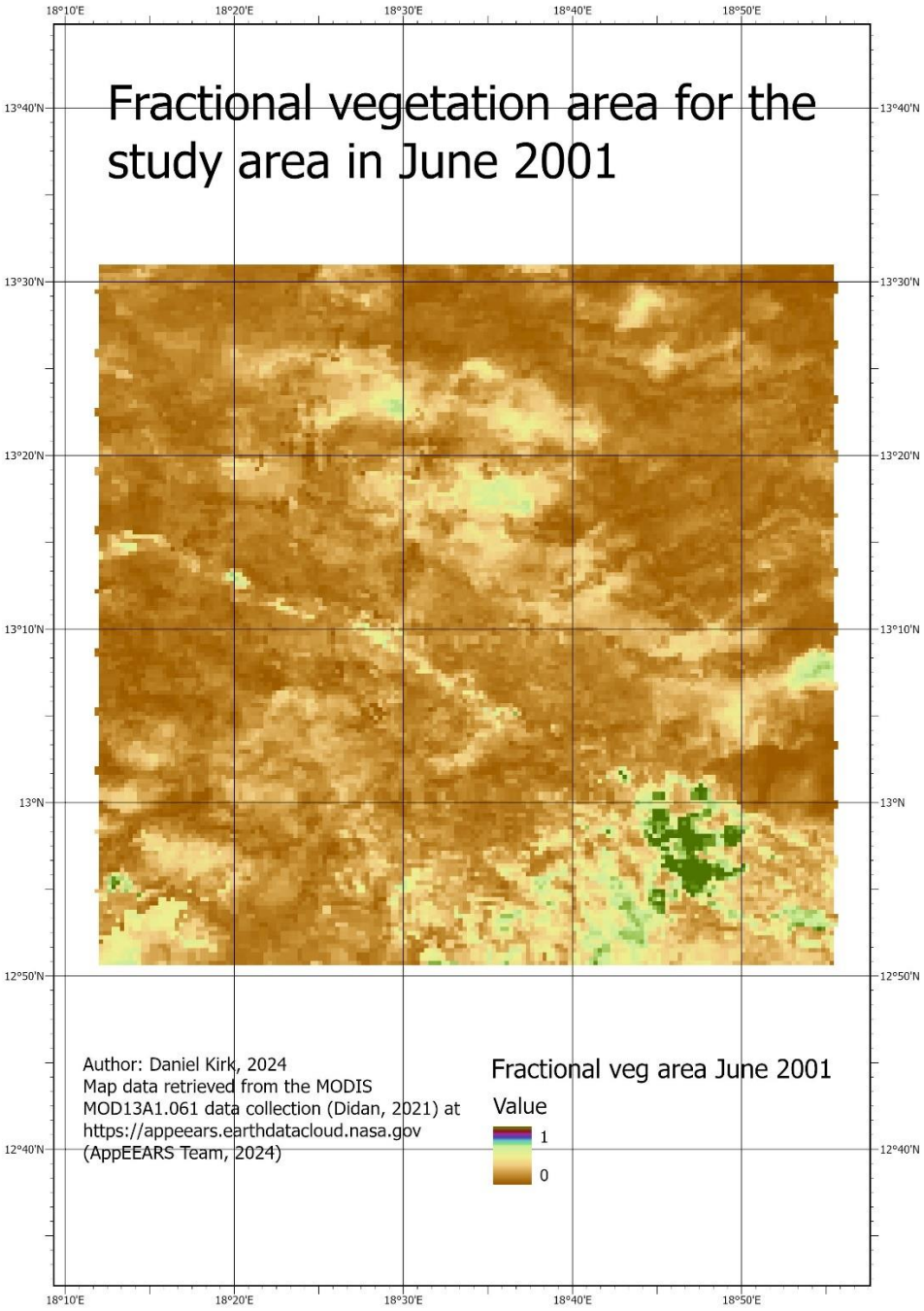

Map 2. Map showing the fractional vegetation area for each 500x500m cell in the study area for June 2001. The map shows the general extent and location of vegetation cover in the study area at the time it was sampled.

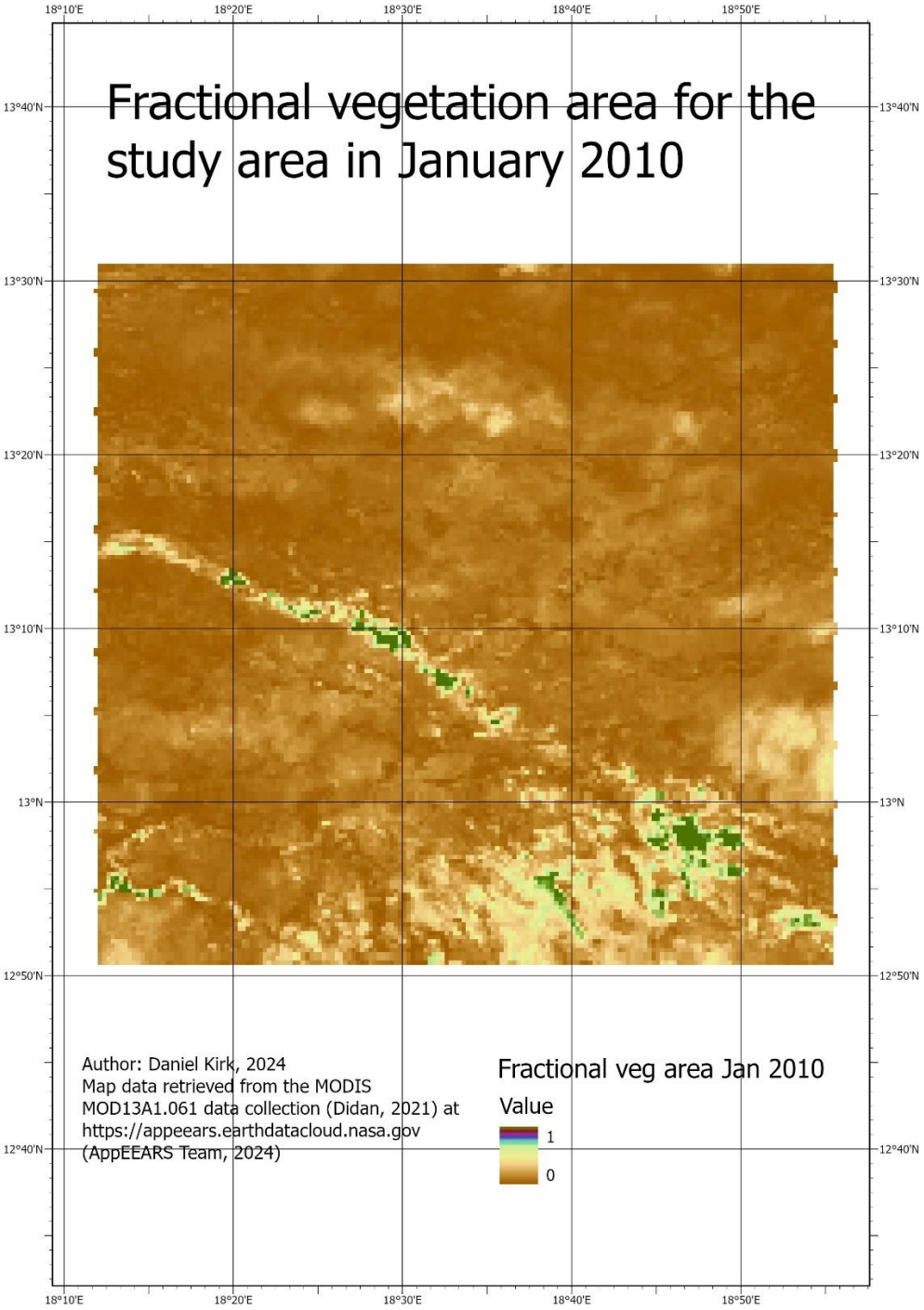

Map 3. Map showing the fractional vegetation area for each 500x500m cell in the study area for January 2010. The map shows the general extent and location of vegetation cover in the study area at the time it was sampled.

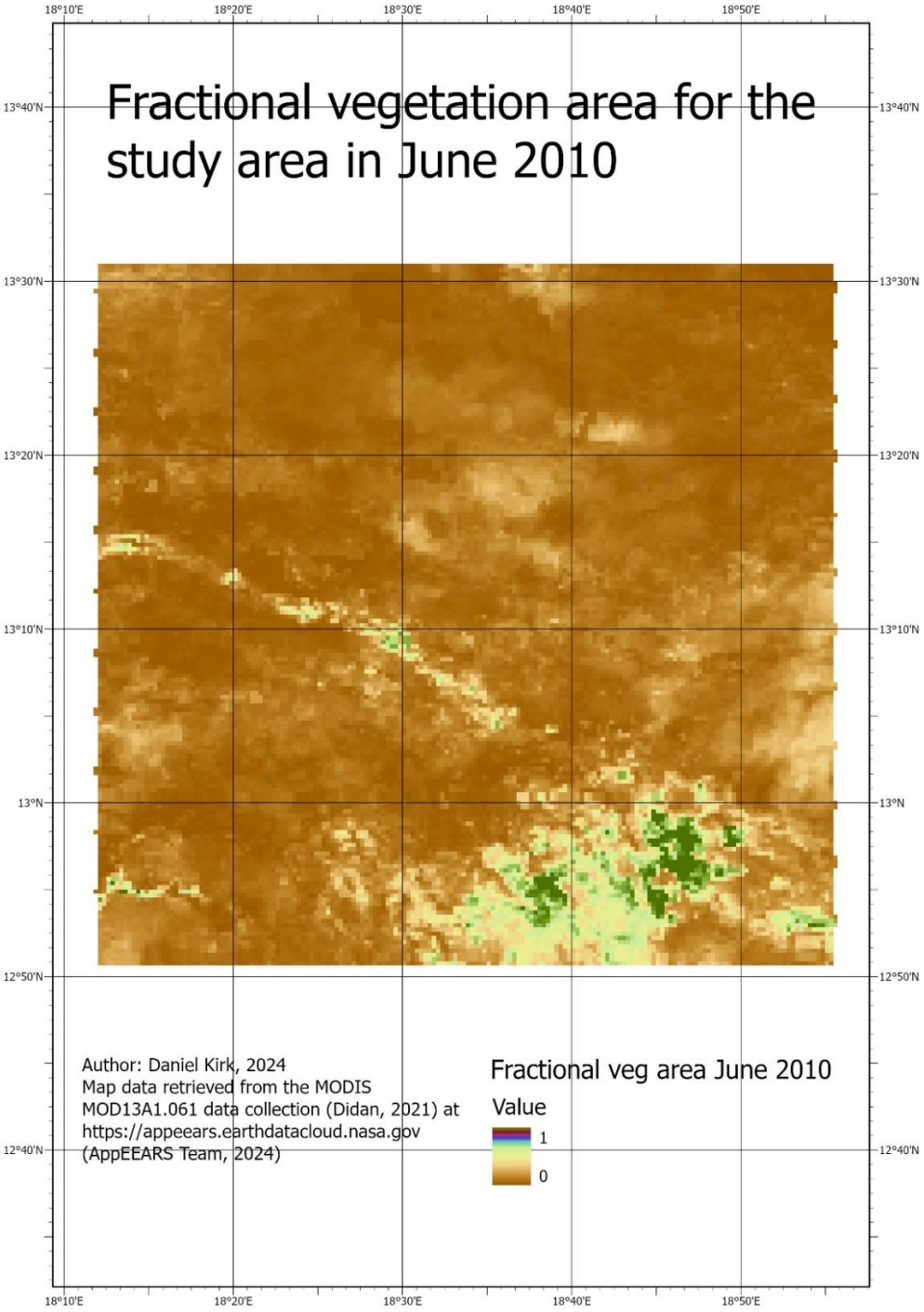

Map 4. Map showing the fractional vegetation area for each 500x500m cell in the study area for June 2010. The map shows the general extent and location of vegetation cover in the study area at the time it was sampled.

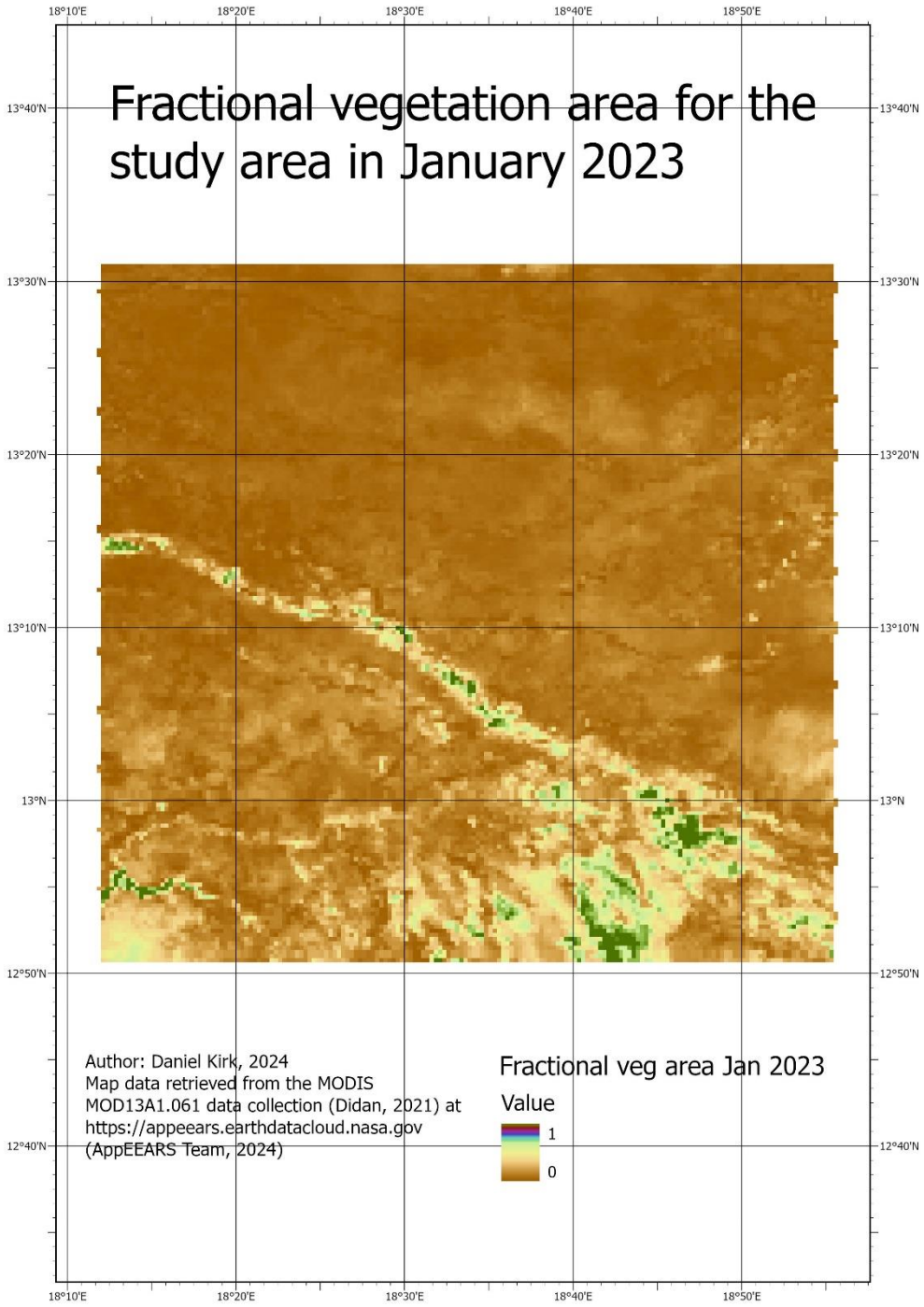

Map 5. Map showing the fractional vegetation area for each 500x500m cell in the study area for January 2023. The map shows the general extent and location of vegetation cover in the study area at the time it was sampled.

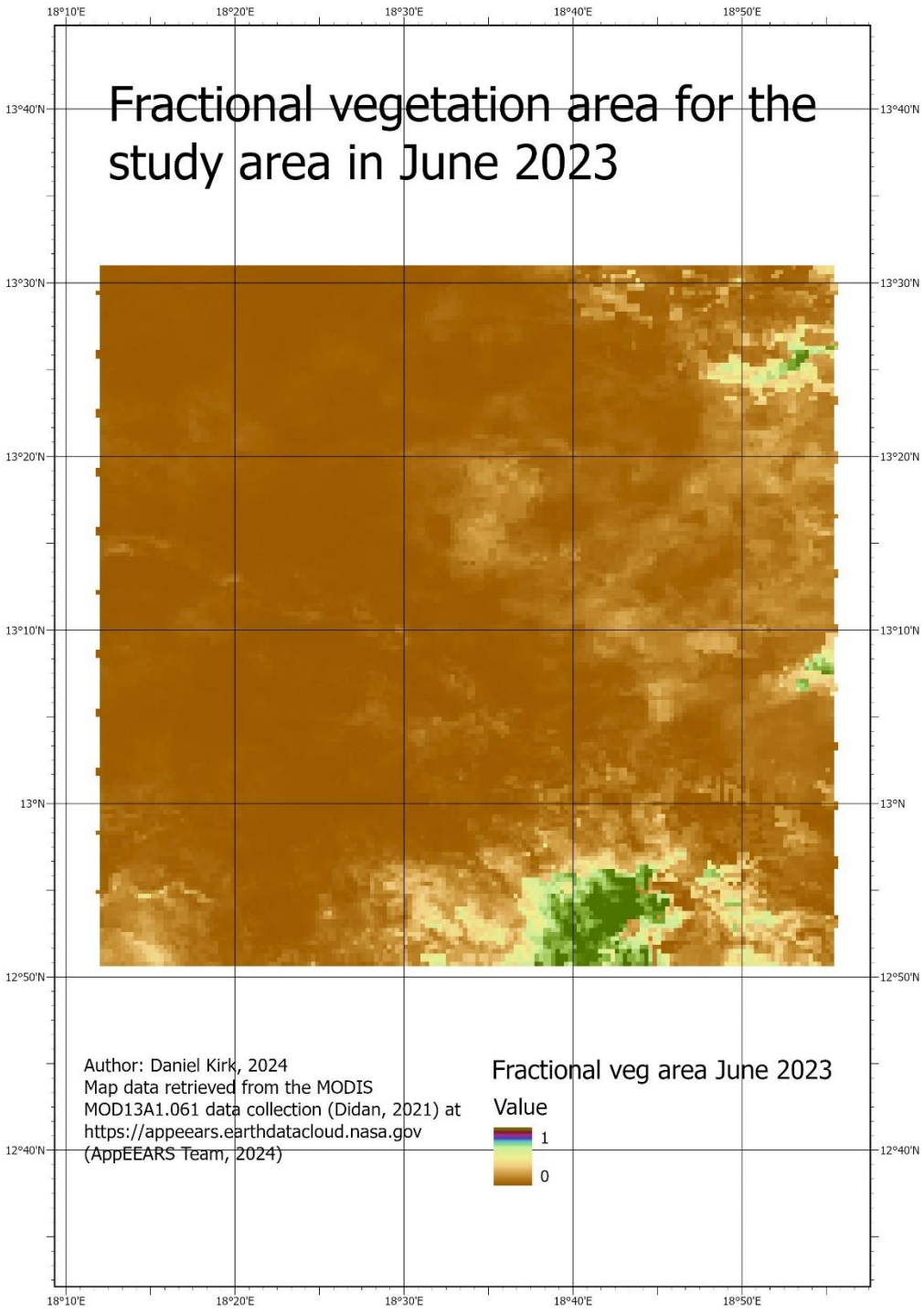

Map 6. Map showing the fractional vegetation area for each 500x500m cell in the study area for June 2023. The map shows the general extent and location of vegetation cover in the study area at the time it was sampled.